Diffusion and Phase Relaxations Within the Interphase Domain of Polymer Blendlike Particles

ÖNDER PEKCAN

Department of Physics, Istanbul Technical University, Maslak, Istanbul, 80626, Turkey

SYNOPSIS

A single-photon counting technique in conjunction with a direct energy transfer (DET) method was used to study the diffusion of small dye molecules within the interphase domain of anthracene (An)- and/or phenanthrane (Phe)-labeled poly(methyl methacrylate) (PMMA) particles sterically stabilized by polyisobutylene (PIB). Mean lifetimes of fluorescing donor molecules were measured during diffusion. A Fickian model for diffusion was employed to fit the experimental data and diffusion coefficients were found to be around 10^{-19} and 10^{-16} cm^2/s at room and above glass transition temperatures (T_g) for the corresponding samples, respectively. A reversed Gaussian distribution was detected for the PMMA phase density at the interphase domain. An increased amount of self-quenching of naphthalene (N) dyes labeled to the PMMA phase was investigated against annealing temperature above T_g and the results were attributed to phase relaxations at the interphase domain. © 1996 John Wiley & Sons, Inc.

INTRODUCTION

The single-photon counting technique for measuring fluorescence decay has been routinely applied to study many blendlike polymeric systems.[1-5] Transient fluorescence spectroscopy with a direct energy transfer (DET) and quenching method has been used to characterize internal morphologies of such composite materials.[6,7] We have reported that the local structure of interpenetrating networklike morphology in latex particles can be studied by the above technique. These latex particles are spherical and usually prepared by dispersion polymerization of methyl methacrylate (MMA) in cyclohexane in the presence of butyl rubber.[8] The major component in this type of particle, a poly(methyl methacrylate) (PMMA) homopolymer of broad molecular weight distribution, is present at about 95% by weight. During the reaction, grafting occurs between the butyl rubber and the growing PMMA chains. Most of the graft copolymer is buried in the particle interior where it forms an interconnected network[2,4] of polyisobutylene (PIB). Some graft copolymer forms a monolayer on the particle surface, which serves as the steric stabilizer. Thus, these particles have an interpenetrating networklike global morphology. This global feature of the morphology has been of interest and studied extensively.[4-6]

In this work, our emphasis is focused on the nature of the interface between the PIB and PMMA phases and their relaxations within the interphase domain.[9] Here, transport experiments involving fluorescence quenching and energy transfer were prepared with nonlabeled and labeled PMMA–PIB particle dispersions in an aliphatic hydrocarbon liquid with free fluorescence dyes. Since this solvent does not swell PMMA itself, we inferred that PIB penetrated throughout the particle, exposing the interior of the particle to solvent. Naphthalene and anthracene derivatives were used as the free fluorescence dyes, diffusing within the interphase domain where the PMMA phase is exclusively labeled either with An or Phe correspondingly. After evaporation of the liquid, we waited for days at room temperature or minutes above the T_g and measured the variation in lifetimes of donor dyes to probe the interphase domain as dye molecules diffuse into particle interior. An experiment with an anthracene (An)-labeled PMMA particle was performed to ob-

served the distribution of the PMMA phase in PIB. DET between diffusing 1-naphthyl methyl pivalate (NMP) and An in the PIB–PMMA interphase domain was detected. Decrease in NMP lifetimes on each consecutive day, at room temperature, suggested that PMMA is distributed in PIB in a reversed Gaussian way. Phenanthrane (Phe)-labeled PMMA particles were used to detect methyl anthracene (MA) diffusion within the interphase domain at 115°C (above T_g). Diffusion coefficients (D) were measured in both experiments and a three orders of magnitude difference was detected between them.

Various types of naphthalene (N)-labeled PMMA particles with different PIB contents were used for annealing experiments to examine phase-relaxation phenomenon within the interphase domain above T_g.

EXPERIMENTAL

Nonlabeled particles were prepared in a two-step process which has previously been described.[1] PIB of a nominal molecular weight of 10,000 was added to a cyclohexane solution of MMA containing azobisisobutyronitrile (AIBN) as a free-radical initiator. The solution was refluxed for several hours to induce polymerization of the MMA. The growing PMMA chains were added across the double bonds present in the PIB to give a graft copolymer soluble in cyclohexane. Polymerization was terminated before the copolymer became insoluble in the cyclohexane solvent. This material, the dispersant, was collected and purified by precipitation with methanol. The dispersant was then added to a second reaction vessel containing MMA and AIBN in cyclohexane. This solution was refluxed overnight. It became increasingly turbid as the reaction progressed. The particles were separated from solvent and unreacted monomers by repeated cycles of centrifugation, decanting the supernatant liquid, and redispersing the particles in fresh solvent. Dispersions in cyclohexane could be freeze-dried and stored as a powder. The powders could be redispersed by subjecting their suspensions in alkane solvents to a few seconds' exposure to an ultrasonic cleaning bath. These particles formed transparent solutions in ethyl acetate and in deuterochloroform. NMR spectra of these latter solutions permitted the composition of the polymers to be determined. (These particles were prepared in Prof. M. A. Winnik's Laboratory in Toronto and provided for our use.)

In this work, two types of unlabeled particles with different PIB content were used. We refer to them as PO3 and PO5. These particles were found to contain 3 and 5 mol % of PIB per gram of polymer, respectively. Naphthalene (N)-labeled particles were also prepared in the way described above and are referred as PN. NMR and UV absorption analysis were used to determine PIB and N content in these particles. Scanning and transmission electron microscopy studies indicated that the particle diameters ranged from 1 to 3 μm. The characteristics of N-labeled and nonlabeled particles are listed in Table I.

An- and Phe-labeled particles were prepared in a two-step process in which MMA in the first step was polymerized to low conversion in isooctane in the presence of PIB containing 2% isoprene units to promote grafting. The graft copolymer produced served as a dispersant in the second stage of polymerization, in which MMA was polymerized in an isooctane solution of the copolymer. Details were reported elsewhere.[10] A stable spherical dispersion of polymer particles were produced of approximately 1 μm in diameter. A combination of NMR and UV analysis indicates that these particles contain 4 monomer mol % PIB and 0.052 mmol An and 0.0072 mmol Phe groups per gram of polymer. We refer to these particles as PA and PP, respectively. Twice recrystallized MA was used as an acceptor for Phe donor during DET processes. PP particles were dispersed in a methylcyclohexane solution of MA in a 13 mm o.d. quartz tube, and then MCH was removed by using a rotary evaporator. MA concentration was measured as 0.15 mmol/g. After this treatment, particles formed a thin film on the inner surface of the quartz tube. The sample was outgassed by blowing nitrogen for 10 min. After sealing, the tube was placed in an oven, where the thin-film sample was annealed at 115°C for various periods of time.

NMP was used as a donor fluorescence dye for diffusion experiments. Transport experiments were prepared by weighing 0.01 g of powder particles (PO3, PO5, or PA) and dispersing them in 0.1 mL methylcyclohexane (MCH) which contains 10^{-3} mol/L NMP, in a 12 mm o.d. quartz tube. Then, the dispersion was placed in a rotary evaporator and MCH was removed at reduced pressure (10 Torr) at 25°C. To get rid of the excess or trapped solvent, samples were left for 24 h in the dessicator, under 10 Torr of pressure. PN samples were prepared in the inner part of the quartz tube in a similar fashion. All samples were purged by dry nitrogen for 10 min to remove the oxygen, before the fluorescence measurements.

Fluorescence decay measurements were carried out by the time-correlated single-photon counting technique employing a pulsed lamp source (Edinburg Instruments, 0.5 atm of D_2 gas) and a Hamamatsu 928 photomultiplier tube. All naphthalene donor samples were excited at 280 nm and emission was detected at 337 nm. The PP sample was excited at 295 nm and emission detected at 345 nm. Fluorescence decay data were collected over 3 decades of decay and fitted by nonlinear least squares using the δ-function convolution method with 2,5-bis(5-tert-butyl-2-benzooxazolyl) thiophene (BBOT) in ethanol as a standard. Data analysis allowed for a small correction due to scattered light (the scatter parameter varied between 0.1 and 1.0). The uniqueness of the fit of the data to the model is determined by χ^2 ($\chi^2 < 1.5$), the distribution of the weighted residuals, and the autocorrelation of the residuals. All measurements were made at room temperature, and since the samples are in powder form, they were positioned so that measurements were made at front-face geometry.

Annealing experiments for the phase relaxation processes were performed with NMP-doped PO3 and PO5 particles. These samples were annealed successively for 1 h periods, at temperatures from 20 to 160°C in an oven under (10 Torr) vacuum. Fluorescence measurements were made at room temperature after each annealing step. Similar annealing experiments were repeated for all PN samples listed in Table I, for phase-relaxation measurements.

RESULTS AND DISCUSSION

Probing Interphase Domain

To probe the interphase domain and to measure diffusion coefficients in this particular region, the fluorescence decay intensity of NMP was fitted to the sum of two exponentials:

$$I(t) = A_1 e^{-t/\tau_1} + A_s e^{-t/\tau_s} \qquad (1)$$

and mean lifetimes were calculated from the relation

$$\langle \tau \rangle = \frac{A_1 \tau_1^2 + A_s \tau_s^2}{A_1 \tau_1 + A_s \tau_s} \qquad (2)$$

where τ_1 and τ_s are the long and short components of lifetimes and A_1 and A_s are the corresponding amplitudes of the decay curves. Lifetime measurements of NMP in the particle interior were taken each consecutive day. Mean lifetimes of NMP in pure PIB and PMMA were found to be 43 and 49 ns, respectively, and it was observed that $\langle \tau \rangle$ values in PO3 increased as time is increased, indicating that NMP molecules traveled from the pure PIB region to the rich PMMA region.[9] The shorter lifetime in PIB compared to PMMA suggested that this polymer is a good quencher for the excited NMP molecule.

A diffusion experiment within the interphase domain in the An-labeled PMMA particle was performed and mean lifetimes of NMP molecules were measured day by day as it diffused into the interphase domain where An are labeled to PMMA. Results are plotted in Figure 1 together with the mean lifetimes of NMP in PO3. Since NMP was already quenched by PIB, corrected mean lifetimes of NMP in the An-labeled particle can be found by normalizing them with NMP lifetimes in PO3. Final results are shown in Figure 2.

It is interesting to note that the curves in Figure 1 are just the reverse of each other, which may suggest that while NMP travels within the interphase domain it transfers its energy to An molecules distributed in the PMMA phase. Intuitively, it is not difficult to conclude that the distribution of An molecules obeyed the reversed Gaussian curve.[9]

Since PMMA is labeled with An molecules, one may suggest that PMMA distribution is just the reverse of PIB distribution in the interphase domain.

Table I Characteristics of Labeled and Nonlabeled Particles Given in the Text

	Nonlabeled Particles		Labeled Particles						
Symbols	PO3	PO5	PN1	PN2	PN3	PN4	PN5	PP	PA
PIB content (mol%)	3	5	7	5	9	9	5	4	4
Dye Concentration (mmol/g)	—	—	0.02	0.15	0.22	0.34	0.45	0.0072	0.052
Labeled with	—	—	N	N	N	N	N	Phe	An
Doped with	NMP	NMP	—	—	—	—	—	MA	NMP
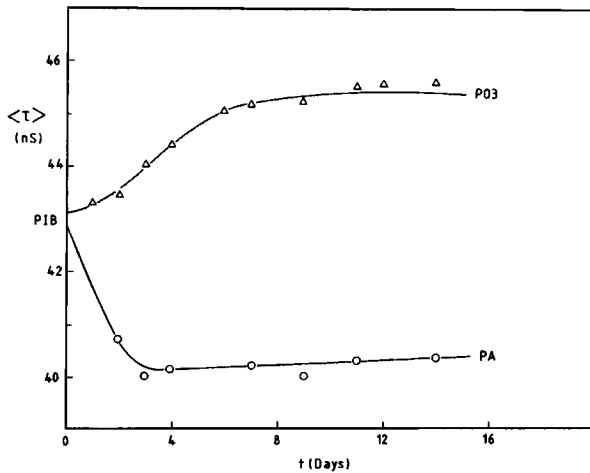
Figure 1 Mean lifetimes of NMP diffusing into (— △ —) PO3 and (— O —) PA particles. Measurements were made on each consecutive day. Lifetime in pure PIB is indicated.

To quantify the above results, a Stern-Volmer-type quenching mechanism may be proposed for the fluorescence decay of NMP in the PMMA–PIB interphase domain of the PA particle where the following law for the lifetime is satisfied[11]:

$$\tau^{-1} = \tau_0^{-1} + k[A] \tag{3}$$

where τ_0 is the lifetime of NMP in pure PMMA in which no quenching has taken place; k, the quenching rate constant; and [A], the An concentration in the region. For low quenching efficiencies, $\tau_0 k[A] \ll 1$, eq. (3) becomes

$$\tau \approx \tau_0(1 - \tau_0 k[A]). \tag{4}$$

The mean lifetime of NMP can be obtained using the following relation:

$$\langle \tau \rangle = \frac{\int_a^r \tau dv}{\int_a^r dv} \tag{5}$$

where dv is the differential volume in the interphase domain and the integral is taken from a to r. Here, if one assumes that the PIB phase distribution in a cylindrical volume follows the Gaussian law,[9] then An (or PMMA) distribution should be given by the following relation:

$$[A] = [A_0](1 - e^{-\alpha(r^2-a^2)}) \tag{6}$$

Here, [A_0] is the An concentration at $r = \infty$, and a is the radius of the cylindrical PIB-rich channel where almost no PMMA exists[9] (see Fig. 3). r is the radial distance from the center and α represents the distribution coefficient for An. According to this picture, at early times, NMP molecules enter the PIB-rich channel; later, NMP molecules emerge from this cylinder to the PMMA-rich region of the interphase domain through thinner PIB channels. Now, the integral in eq. (5) for $r > a$ can be solvend and the result is found to be

$$\frac{\langle \tau \rangle}{\tau_0} = 1 - \tau_0 k[A_0]\left[1 + \frac{(e^{-\alpha(r^2-a^2)} - 1)}{2\alpha(r^2 - a^2)}\right] \tag{7}$$

In this model, NMP molecules emerging from the cylindrical source can travel an average distance r at time t. This relation can be given by the following formula[12]:
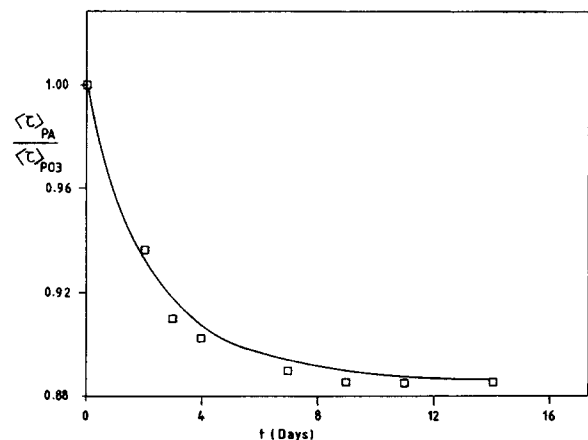
$$r = \sqrt{\frac{4Dt}{\pi}} \tag{8}$$

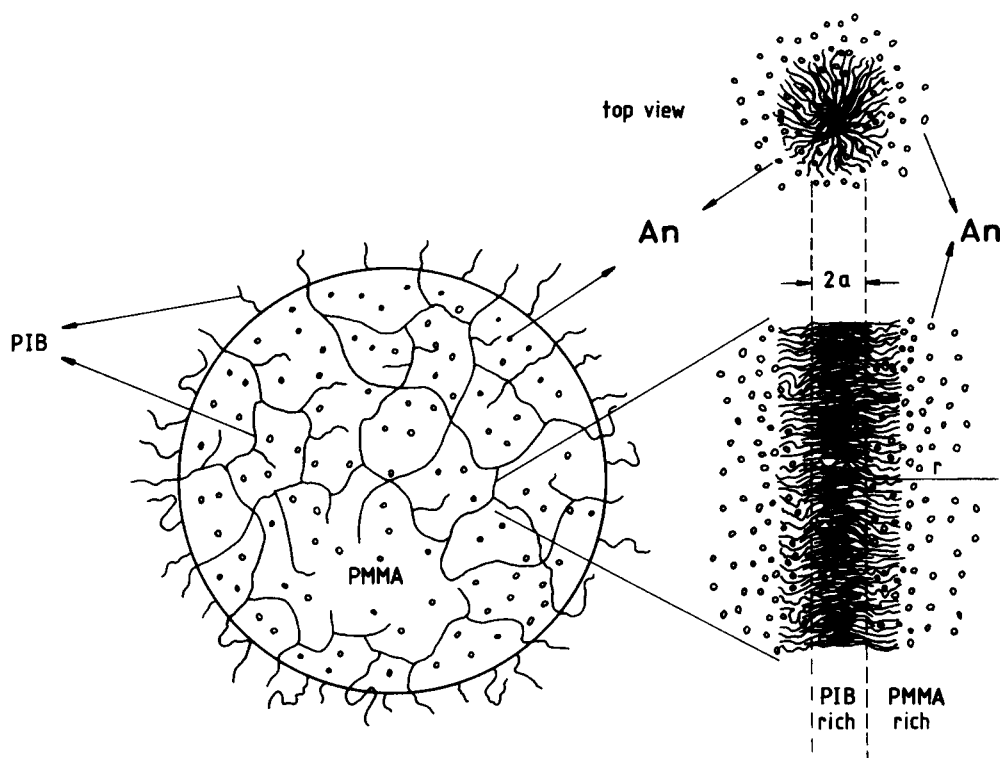where D is the diffusion coefficient for the NMP molecules. Now, eq. (7) is written as

$$\frac{\langle \tau \rangle}{\tau_0} = 1 - c + \frac{c(1 - e^{-\beta(t-t_a)})}{2\beta(t - t_a)} \tag{9}$$

Here,

$$C = \tau_0 k[A_0], \quad \beta = \alpha\frac{4D}{\pi}, \quad t_a = \frac{\pi a^2}{4D} \tag{10}$$

Figure 2 Normalized mean lifetimes of NMP diffusing into An-labeled particle (PA). $\langle \tau \rangle_{PA}$ and $\langle \tau \rangle_{PO3}$ are the mean lifetimes of NMP in PA and PO3 particles, respectively.

Figure 3 Cartoon representation of An-labeled PMMA-PIB particle with the magnified part of the interphase domain. a is the radius of the cylindrical PIB-rich channel.

Equation (9) can be fitted to the normalized mean lifetimes of NMP in Figure 2. A quite successful fit is found, and calculated fitting parameters are listed in Table II for the PA particles.

The magnitude of the measured diffusion coefficient (3.55×10^{-19} cm^2/s) is quite reasonable for a small molecule diffusing within the polymeric environment at room temperature. We have previously found $D = 10^{-15}$ cm^2/s for a solvent molecule penetrated into nonaqueous dispersion particles of same type[13] at room temperature.

Using eq. (6) and the experimentally obtained α value, the distribution of the An-labeled PMMA phase in the interphase domain is obtained and plotted in Figure 4 for the PA particle. Here, it is interesting to note that the NMP molecule traveled

in the PMMA-rich region for almost 15 days; even the distance is much shorter than in the PIB-rich region. This can be understood by assuming the existence of very thin PIB microchannels in the glassy PMMA phase in which NMP can diffuse. Cartoon representation of the whole morphology of the interphase domain is already shown in Figure 3.

Diffusion Above T_g

Typical fluorescence decay curves for Phe-labeled PMMA particle are presented in Figure 5 with and without MA (acceptor). Decay of the Phe fluorescence with no MA is exponential in curve a, with a lifetime of $\tau_0 = 44$ ns. However, in curve b, Phe decay deviates from exponentiality for PP particles

Table II C, β, and t_a Values Obtained from Curve Fitting to Eq. (9) and D and α Values Calculated from Eq. (10), Where a is Taken from Ref. 4.

| Particle	C	β	t_a	D (cm^2/s)	α (A°)$^{-2}$
PA	0.12	0.75 (day^{-1})	1.6 (day)	3.55×10^{-19}	$1.28/a^2$
PP	0.21	0.32 (min^{-1})	4.0 (min)	2.04×10^{-16}	$1.28/a^2$
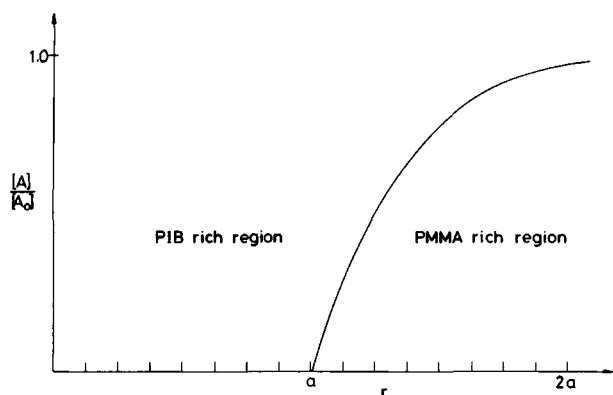
Figure 4   Plot of [A] function [eq. (6)] for PA particle $(\alpha = 1.28)$.

doped with MA and annealed at 115°C for 15 min. These curves can be fitted to eq. (1) to obtain decay parameters. Using eq. (2), mean lifetimes of Phe of PP samples annealed at elevated time intervals at 115°C were obtained. Then, eq. (9) is used to fit these experimentally obtained $\langle\tau\rangle/\tau_0$ ratios to find C, β, and t_a values. Now, [A$_0$] in eqs. (9) and (10) represents the MA concentration in the region. A fit is presented in Figure 6 and the measured parameters are listed in Table II. The observed value of the diffusion coefficient, $D = 2.04 \times 10^{-16}$ cm^2/s, is found to be three orders of magnitude larger than the value obtained at room temperature and one order of magnitude smaller than the D value of the solvent molecule diffusing into similar environment.[13] Here, we believe that the plastisizing effect is more pronounced than is the temperature effect in such systems. We have also to note that the Phe labeled to PMMA here, in fact, probes the MA molecules traveling within the interphase domain at each annealing step.
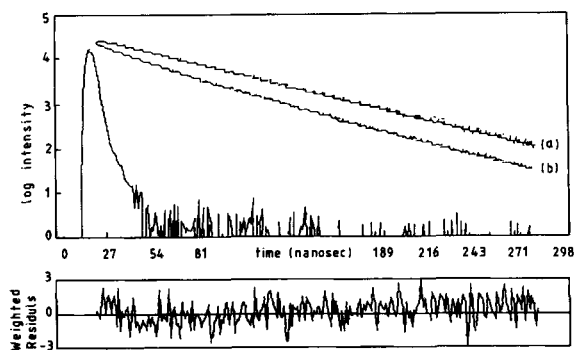

Figure 5   Fluorescence decay of (a) Phe in PP particles with no MA ($\tau_0 = 44$ ns) and (b) Phe after annealing of PP particles with MA at 115°C for 15 min.
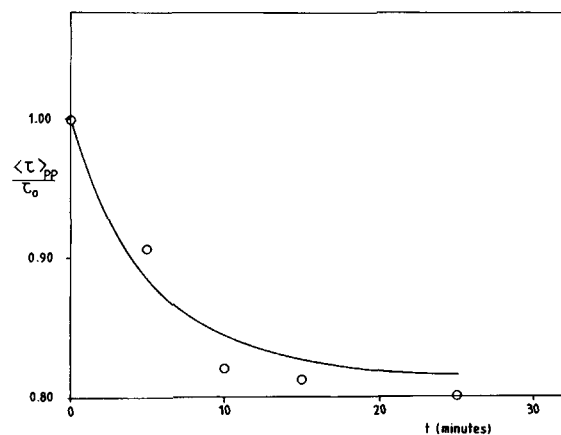
Figure 6   Plot of normalized mean lifetimes of Phe in MA-doped PP particles, annealed at elevated time intervals at 115°C temperature. $\tau_0 = 44$ ns is taken as the Phe lifetime with no MA. (All measurements were taken at room temperature after each annealing step.)
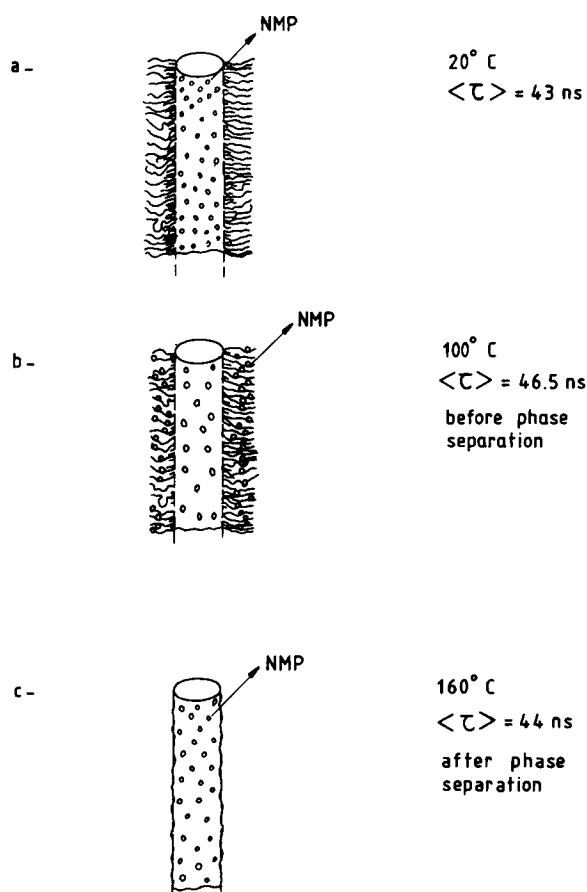
Phase Separation due to Annealing

Mean lifetimes $\langle\tau\rangle$ obtained from eq. (2) for NMP-doped PO3 and PO5 samples annealed at temperatures from 20 to 160°C are plotted in Figure 7. $\langle\tau\rangle$ values increase as the annealing temperature is increased and reach the maximum value around 100°C, then decrease as the temperature is increased for both samples. The measured mean lifetimes of NMP in the PO3 sample presented larger values than those of the PO5 sample. These peculiar behaviors of the $\langle\tau\rangle$ values may be explained by the "phase relaxation" within the interphase domain.
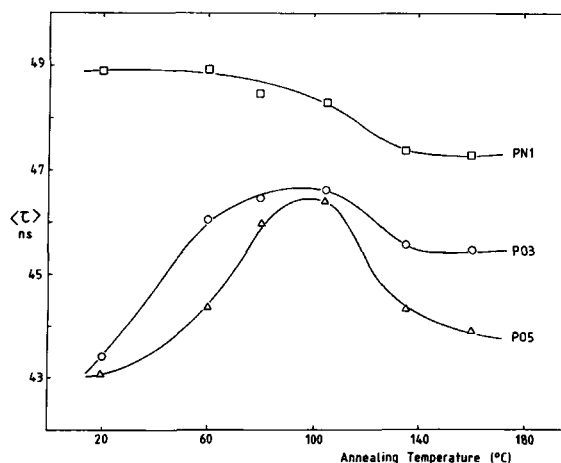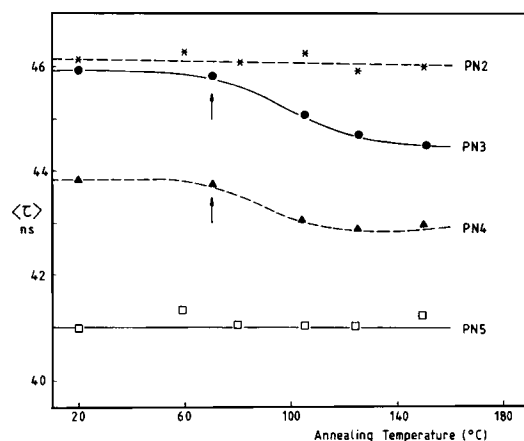

Figure 7   Variation of mean lifetimes of NMP due to annealing of PO3 and PO5 particles at elevated temperatures. Mean lifetimes of N-labeled particles (PN1) are also given for comparison.

Initially, NMP molecules are located in the PIB-rich region; later, due to annealing of polymer particles around the T_g of PMMA, NMP molecules are forced to diffuse into PIB microchannels within the PMMA phase where the lifetime of NMP is much larger. Further, annealing of these particles much above T_g may cause complete phase separation of PIB and PMMA components in the interphase domain. Most probably, NMP molecules remain in the PIB phase, which present smaller $\langle \tau \rangle$ values. The cartoon representation of the phase-separation process in the interphase domain of PO3 and PO5 particles is depicted in Figure 8.

On the other hand, due to annealing of N-labeled PMMA particles, $\langle \tau \rangle$ values presented different behavior from that of unlabeled particles. Plots of $\langle \tau \rangle$ vs. annealing temperature are shown in Figure 9 for PN samples with various PIB content and increasing amount of naphthalene concentration. $\langle \tau \rangle$ values in particles with high PIB content showed a decrease

Figure 9   Variation of mean lifetimes of N due to annealing of N-labeled PMMA particles at elevated temperatures. (characteristics of PN particles are given in Table I).

Figure 8   Cartoon representation of phase separation process in the interphase domain during annealing of PO3 and/or PO5 particles: (a) below, (b) around, and (c) well above T_g (105°C).

above 60°C annealing temperature, which then was saturated due to further annealing at higher temperatures. In particles with lower PIB content, however, $\langle \tau \rangle$ values remain constant at all temperatures. Variations in mean lifetimes of PN particles for a given N concentration ([N]) can be explained by the phase relaxations in the interphase domain.

Presumably, before annealing, the existence of PIB microchannels in the PMMA phase may cause dilution of the [N] concentration, which provides larger $\langle \tau \rangle$ values. Annealing of PN samples above T_g caused phase separation between PMMA and PIB, which then resulted contraction in the PMMA phase. These processes increase [N] in the region; as a result, $\langle \tau \rangle$ values decrease. The sensitivity of lifetimes to N groups in the PMMA phase can be quantitatively understood by the self-quenching equation

$$N^* + N \rightarrow 2N \qquad (11)$$

which leads to dissipation of electronic excitation of N* molecules to heat. Decrease in the mean separation of N groups increase the extend of self-quenching and mean lifetimes of N may become shorter. Cartoon representation of phase separation in PN particles is shown in Figure 10.

Self-quenching of N in the PMMA Phase

$\langle \tau \rangle$ values from Figure 9 are plotted vs. [N] concentration before and after annealing in Figure 11, where one can observe two straight lines with different slopes. To explain these observations, we em-
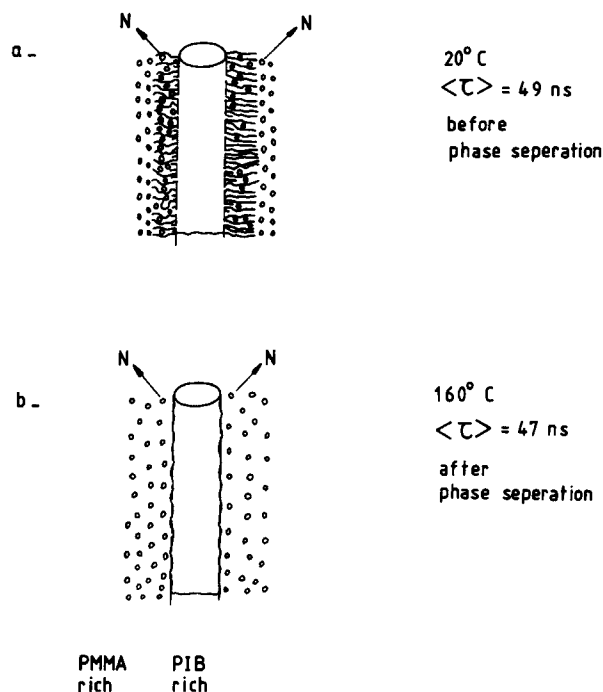
Figure 10   Cartoon representation of the phase-separation process in the interphase domain during annealing of rich PIB contained N-labeled PMMA particle (PN1): (a) below and (b) well above T_g (105°C).

ployed Inokuti–Hirayama's (IH)[14] model which is based Dexter's theory of energy transfer by an exchange mechanism.[15] In this model, the rate constant, k_q, for quenching depends upon the distance R between N* and the quencher, which is given by the following formula:

$$k_q(R) = \frac{1}{\tau_0} \exp[\gamma(1 - R/R_0)] \qquad (12)$$

Here, τ_0 is the excited-state lifetime in the absence of a quencher, R_0 is the critical transfer radius, and $\gamma = 2R_0/L$, where L is the effective average Bohr radius. Note that in the presence of a quencher, when $R = R_0$, $k_q(R) = 1/\tau_0$ and quenching occurs with 50% efficiency. Based upon this model, IH showed that the intensity of the excited state, $I(t)$, should decay as

$$I(t) = I_0\exp[-t/\tau_0 - [N]/[N_0]] \qquad (13)$$

where $[N_0] = 3 \times 10^{27}/4\pi(R_0)^3 N_A$, with R_0 in angstroms and N_A is Avogadro's number. The mean decay time $\langle \tau \rangle$ can be shown to depend upon [N] according to
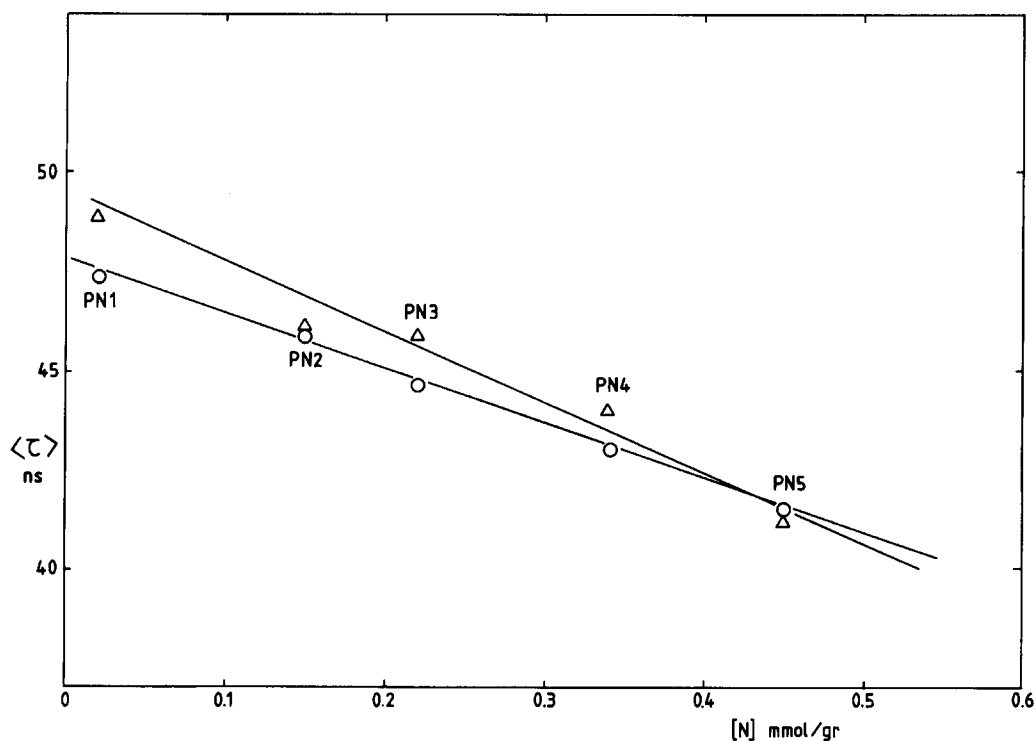
Figure 11   Plot of mean lifetimes from Figure 9 vs. naphthalene concentration [N] in N-labeled particles (PN1, PN2, PN3, PN4, and PN5): (— O —) before (20°C) and (— △ —) after (150°C annealing).

$$\langle\tau\rangle/\tau_0 = [1 - [N]/[N_0]) \qquad (14)$$

To derive the above equation, IH was applied the Perrin's "active sphere" model[15] with the following boundary conditions:

$$k_q(r) = \begin{matrix} \infty & R < R_0 \\ 0 & R_0 < R \end{matrix} \qquad (15)$$

When eq. (14) is fitted to experimental data in Figure 11, $[N_0]^{-1} = 0.37$ and 0.28 were obtained before and after annealing processes, respectively. These values produced $R_0 = 5.27$ and 4.80 Å for the corresponding data. Here, a smaller R_0 value compared to previous ones supports the idea of a phase-separation process after annealing the labeled samples above T_g at 150°C, at which self-quenching between N* and N molecules increase due to a decrease in distance between them. One may have to note that the magnitude of experimentally obtained R_0 values are quite reasonable for the energy-transfer process by the electron-exchange mechanism.

REFERENCES

1. Ö. Pekcan, M. A. Winnik, and M. D. Croucher, *Macromolecules*, **16**, 699 (1983).
2. Ö. Pekcan, M. A. Winnik, and M. D. Croucher, *J. Polym. Sci. Polym. Lett.*, **21**, 1011 (1983).
3. Ö. Pekcan, M. A. Winnik, and M. D. Croucher, *Phys. Rev. Lett.*, **61**, 641 (1988).
4. Ö. Pekcan, L. S. Egan, M. A. Winnik, and M. D. Croucher, *Macromolecules*, **23**, 2210 (1990).
5. Ö. Pekcan, *Chem. Phys. Lett.*, **20**, 198 (1992).
6. Ö. Pekcan, M. A. Winnik, and M. D. Croucher, *Chem. Phys.*, **146**, 283 (1990).
7. Ö. Pekcan, *Chem. Phys.*, **177**, 619 (1993).
8. M. A. Winnik, in *Polymer Surfaces and Interfaces*, J. Feast and H. Munro, Eds., Wiley, London, 1983, Chap. 1.
9. Ö. Pekcan, *J. Appl. Polym. Sci.*, **49**, 151 (1993).
10. M. A. Winnik, Ö. Pekcan, L. Chen, and M. D. Croucher, *Macromolecules*, **21**, 55 (1988).
11. J. B. Birks, *Photo Physics of Aromatic Molecules*, Wiley-Interface, New York.
12. J. Crank, *Mathematics of Diffusion*, 2nd ed., Clarendon Press, Oxford, 1975.
13. Ö. Pekcan and Y. Demir, *J. Appl. Polym. Sci.*, **43**, 2169 (1991).
14. M. Inokuti and F. Hirayama, *J. Chem. Phys.*, **43**, 1978 (1965).
15. D. L. Dexter, *J. Chem. Phys.*, **21**, 836 (1953).